International Journal of Bifurcation and Chaos, Vol. 32, No. 5 (2022) 2250063 (20 pages)

DOI: 10.1142/S0218127422500638

Hidden and Self-Excited Collective Dynamics of a New Multistable Hyper-Jerk System with Unique Equilibrium

M. D. Vijayakumar
Centre for Material Research,
Chennai Institute of Technology, Chennai, India

Hayder Natiq
Information Technology College,
Imam Ja'afar Al-Sadiq University, 10001, Baghdad, Iraq

Gervais Dolvis Leutcho*
Department of Electrical Engineering,
École de Technologie Supérieure (ÉTS),
Montréal, Québec H3C1K3, Canada
leutchoeinstein@yahoo.com

Karthikeyan Rajagopal
Centre for Nonlinear Systems,
Chennai Institute of Technology, Chennai, India

Sajad Jafari
Health Technology Research Institute,
Amirkabir University of Technology (Tehran Polytechnic), Iran
Department of Biomedical Engineering,
Amirkabir University of Technology (Tehran Polytechnic), Iran

Iqtadar Hussain
Mathematics Program, Department of Mathematics,
Statistics and Physics, College of Arts and Sciences,
Qatar University, 2713, Doha, Qatar

Received May 31, 2021; Revised September 10, 2021

Nonlinear dynamical systems with hidden attractors belong to a recent and hot area of research. Such systems can exist in different forms, such as without equilibrium or with a stable equilibrium point. This paper focuses on the dynamics of a new 4D chaotic hyper-jerk system with a unique equilibrium point. It is shown that the new hyper-jerk system effectively exhibits different hidden behaviors, which are hidden point attractor, hidden periodic attractor, and hidden chaotic state. Collective behaviors of the system are studied in terms of the equilibrium point, bifurcation diagrams, phase portraits, frequency spectra, and two-parameter Lyapunov exponents. Some remarkable and exciting properties are found in the new snap system, such as period-doubling transition, asymmetric bubbles, and coexisting bifurcations. Also, we demonstrate that it is possible to generate different varieties of two, three, four, or five coexisting hidden and self-excited attractors in the introduced model. In addition, the amplitude and offset of the hidden

*Author for correspondence

chaotic attractors are perfectly controlled for possible application in engineering. Furthermore, a circuit design has been implemented to support the physical feasibility of the proposed model.

Keywords: Hyper-jerk system; stable equilibrium; hidden attractor; multistability; control.

1. Introduction

Nonlinear problems are of interest to mathematicians, physicists, and other scientists because most physical systems are nonlinear. Complex phenomena, including chaos, can be observed when modeling some natural physical systems, such as a Hybrid Electric Vehicle (HEV) [Meli *et al.*, 2021; Tametang Meli *et al.*, 2021] or electrical hair clippers [Hu *et al.*, 2018a; Hu *et al.*, 2018b; Nana *et al.*, 2018], just to name a few. In artificial neural networks, for example, nonlinearities can be deliberately introduced to allow certain calculations. Under certain conditions, nonlinear systems exhibit sensitivity to initial values (IC), intermittency, and chaos [Strogatz, 1994]. In a nonlinear dynamical system, chaotic behavior is the fingerprint of at least one positive Lyapunov exponent. Such behavior has been found in several categories of systems, including physical, biological, ecological systems, electronic circuits, mechanical systems, and so on [Strogatz, 1994; Bao *et al.*, 2020a]. Notice that although most chaotic systems are of hyperbolic type, there are still many that are not. In other words, it will be surprising to show that systems with only one stable equilibrium exhibit chaos. For this particular class of system, one would almost certainly expects asymptotically convergent behaviors. In this regard, Wang and Chen [2012] presented a surprising possibility of finding autonomous quadratic chaotic systems with only one stable equilibrium. Since this discovery, other interesting chaotic systems with one stable equilibrium have been reported and investigated [Pham *et al.*, 2017]. Such systems from the viewpoint of computation have been classified as systems with hidden attractors. From a computational perspective, systems with stable equilibrium have been classified as systems with hidden attractors [Leonov & Kuznetsov, 2013]. Remember that if the basin of attraction for the attractor does not intersect with small neighborhoods of any equilibrium points, then that strange attractor is hidden. Otherwise, it is self-excited [Leonov *et al.*, 2015]. This topic of chaotic systems with hidden strange attractors has been the subject of various discussions and research in the scientific community. Other chaotic systems in which hidden strange attractors occur are systems with infinite equilibria, stable or no equilibria, as discussed in [Yu *et al.*, 2020; Zhang *et al.*, 2019; Chen *et al.*, 2020]. Also, systems with multistability [Bao *et al.*, 2020b], megastability [Giakoumis *et al.*, 2020; Jafari *et al.*, 2019; He *et al.*, 2018], and extreme multistability [Chen *et al.*, 2019] are of noticeable interest.

In a mechanical system, the derivative of the position gives velocity, the second derivative of the position gives acceleration, and the derivative of acceleration gives jerk. This is why jerk systems [Malasoma, 2000] are expressed as $\dddot{x} = J(\ddot{x}, \dot{x}, x)$, where $J = (\cdot)$ is called the "*jerk function*". For such jerk system, several have already been reported in the literature, and the results have indicated some very rich and striking phenomena, including symmetric properties, Hopf bifurcation, symmetry-breaking, symmetry bubbles, period-doubling scenario, the coexistence of multiple bifurcations mode, and coexistence of multiple attractors [Kengne *et al.*, 2020b]. Thus in jerk systems, an extensive repertoire of nonlinear behavior is recorded. In the literature [Leutcho *et al.*, 2018; Munmuangsaen & Srisuchinwong, 2011], the fourth time derivative d^4x/dt^4 is called a "*snap*". Hyper-jerk systems are classified as high-order dynamical systems but have the mathematical distinction of having a "*simple*" and "*elegant*" structure. For these reasons, new hyper-jerk systems/circuits capable of generating both series and parallel bubbles of bifurcation are introduced and analyzed in recent years [Leutcho *et al.*, 2020a; Leutcho *et al.*, 2020b]. The authors generated such complicated behaviors (i.e. coexisting bubbles, bursting oscillations, and so on) by introducing exponential nonlinear terms into the mathematical model. In 2018, Ren *et al.* [2018] introduced the first hyper-jerk chaotic system with nonlinear quadratic terms and having hidden dynamics. They exploited well-known dynamical tools to investigate its dynamics in its fractional order. Very recently,

Table 1. Characterization of reported chaotic systems with specific equilibrium points and the number of coexisting attractors.

Nature of the Hyper-Jerk Chaotic System	Type of Attractors	Number of Coexisting Attractors	Number of Nonlinear Terms	References
4D with no equilibrium point	Hidden	×	04	[Ren *et al.*, 2018]
4D with a stable equilibrium point	Hidden	02	03	[Singh *et al.*, 2018]
4D with a unique equilibrium point	Hidden and Self-excited	02, 03, 04, 05	02	This work

Fouodji Tsotsop *et al.* [2020] examined a new hyper-jerk system with three equilibria. The authors have explored the dynamic properties of the proposed system with hyperbolic sine nonlinearity. Also, the case reported in their work represents a unique one that displays the coexistence of stable fixed points and self-excited chaotic attractors. It is observed from Table 1 that no 4D hyper-jerk system with up to five coexisting hidden attractors and two nonlinear terms was proposed in the literature. To the best of the authors' knowledge, the introduced hyper-jerk system represents the unique and "*elegant*" model with only one equilibrium point that can show a plethora of coexisting hidden and self-excited states.

This paper is structured as follows. Section 2 is concerned with the system description. Some properties of the system, such as fixed points, stability, and dissipation, are examined. Bifurcation analysis, route to chaos, and two-parameter Lyapunov exponents are analyzed in Sec. 3. Also, coexisting bifurcations, multistability, offset boosting control, total amplitude control, and antimonotonicity are analyzed. The feasibility of the proposed system on PSIM (Power Simulation) based simulation is carried out in Sec. 4. A concluding remark is presented in Sec. 5.

2. The 4D Hyper-Jerk System

2.1. *Model description*

In this paper, the mathematical model of a new 4D autonomous hyper-jerk system is introduced. The model is expressed by the differential Eq. (1)

$$\begin{cases} \dot{x} = y, \\ \dot{y} = z, \\ \dot{z} = w, \\ \dot{w} = -ax - by - cw - dy^2 + exz - f, \end{cases} \tag{1}$$

where x, y, z, and w are the state variables; a, b, c, d, e, and f are six positive real constants with one bias term, which is f. It is clear that the new model possesses only two quadratic nonlinear terms, which can be implemented easily with analog multiplier chips. Furthermore, no apparent symmetry can be observed from Eq. (1) despite the presence of quadratic nonlinearities since the model is variable under the substitution $(x, y, z, w) \rightarrow (-x, -y, -z, -w)$. More importantly, the new hyper-jerk oscillator Eq. (1) can be considered in the general hyper-jerk form as follows:

$$\frac{d^4x}{dt^4} = -ax - b\frac{dx}{dt} - c\frac{d^3x}{dt^3} - d\left(\frac{dx}{dt}\right)^2 + ex\frac{d^2x}{dt^2} - f. \tag{2}$$

2.2. *Dissipation*

Dissipation (i.e. volume contraction) is a common property in nonlinear dynamical systems. This dissipation is used to show if the phase space is conserved or not. An attractor can be characterized in nonlinear systems by calculating its dissipation. That is, if and only if this dissipation is negative. In this section, the dissipation is calculated using the definition as

$$\Lambda = \frac{\partial \dot{x}}{\partial x} + \frac{\partial \dot{y}}{\partial y} + \frac{\partial \dot{z}}{\partial z} + \frac{\partial \dot{w}}{\partial w} = -c. \tag{3}$$

We clearly remark that the volume contraction is negative since coefficient c is positive. Thus, the new hyper-jerk system with its unique fixed point is dissipative and presents attractors.

2.3. *Equilibrium points and stability*

Let $\dot{x} = \dot{y} = \dot{z} = \dot{w} = 0$ then, the equilibrium points of (1) is calculated as: $E\{(x^*, y^*, z^*, w^*) \,|\, x^*\} = -f/a; y^* = z^* = w^* = 0$. Thus the hyper-jerk

Table 2. Eigenvalues $\lambda_j\{j = 1, 2, 3, 4\}$ of equilibrium point $E(-f/a, 0, 0, 0)$ for $b = 0.54$, $f = 2.39$, $c = 0.54$, $d = 1.07$, $e = 1.97$.

a	$\lambda_{1,2}$	$\lambda_{3,4}$	Natures
0.1	$-0.2643 \pm i6.8560$	$-0.0057 \pm i0.0457$	Stable saddle-focus
0.52	$-0.2415 \pm i2.9851$	$-0.0285 \pm i0.2391$	Stable saddle-focus
1	$-0.2204 \pm i2.0954$	$-0.0496 \pm i0.4720$	Stable saddle-focus
1.45	$-0.2119 \pm i1.6143$	$-0.0581 \pm i0.7373$	Stable saddle-focus
1.6	$-0.2207 \pm i1.4522$	$-0.0493 \pm i0.8597$	Stable saddle-focus
1.8	$-0.3469 \pm i1.2128$	$0.0769 \pm i1.0608$	Unstable saddle-focus
3.5	$-0.9226 \pm i1.0844$	$0.6526 \pm i1.1405$	Unstable saddle-focus

model depicted in (1) possesses a unique equilibrium point. The Jacobian matrix of the new 4D hyper-jerk system evaluated at any equilibrium $E(x^*, y^*, z^*, w^*)$ is given by,

$$J = \begin{bmatrix} 0 & 1 & 0 & 0 \\ 0 & 0 & 1 & 0 \\ 0 & 0 & 0 & 1 \\ -a + ez^* & -b - 2dy^* & ex^* & -c \end{bmatrix}. \quad (4)$$

The eigenvalues of the Jacobian matrix J are the roots of the characteristic equation $|J - \lambda I_d| = 0$, where I_d is the 4×4 identity matrix and λ the eigenvalues, which can be calculated as

$$\lambda^4 + c\lambda^3 + \frac{ef}{a}\lambda^2 + b\lambda + a = 0. \quad (5)$$

Consider the following polynomial

$$p^4 + m_3p^3 + m_2p^2 + m_1p + m_0 = 0. \quad (6)$$

All the roots of the real parts of Eq. (6) are negative according to the Routh–Hurwitz stability method [Zambrano-Serrano & Anzo-Hernández, 2021] if and only if the following conditions are satisfied

$$m_i > 0 \quad (i = 0, 1, 2, 3),$$

$$m_1m_2m_3 - m_1^2 - m_0m_3^2 > 0.$$

From the above condition, we obtained the sufficient condition of stability of the characteristic polynomial (5) and thus of the unique fixed point $E(x^*, y^*, z^*, w^*)$ accordingly as

$$a, b, c > 0, \quad \frac{ef}{a} > 0 \quad \text{and,} \quad b^2 + ac^2 > \frac{cbef}{a}.$$

So, if the system (1) is stable, we confirm that the system belongs to the category of hidden attractors with a stable equilibrium point. Based on Eq. (5), we have provided Table 2 showing various behaviors (hidden/self-existed) that can be found in a new hyper-jerk system under consideration.

3. Nonlinear Dynamics of the Oscillator

3.1. *Bifurcation analysis and route to chaos*

The dynamics of the new hyper-jerk system (1) are numerically analyzed in this section using a fourth-order Runge–Kutta integrator with a fixed time grid $\Delta t = 3 \times 10^{-3}$. The diagrams of bifurcation and graphs of Lyapunov exponents are two main tools that are presented to gain more information about different behavior to chaos in the new 4D chaotic hyper-jerk system when parameters are changed. The bifurcation diagram of the system represents the plot of the local maxima of the variable x or w in terms of the control parameter a and f. At the same time, the graphs of Lyapunov exponents are obtained using the algorithm proposed by Wolf and co-workers [Wolf *et al.*, 1985]. Sample results are provided in Figs. 1 and 2. In particular, Fig. 1 shows different paths related to the system's dynamics, considering the variation of the parameter a in the

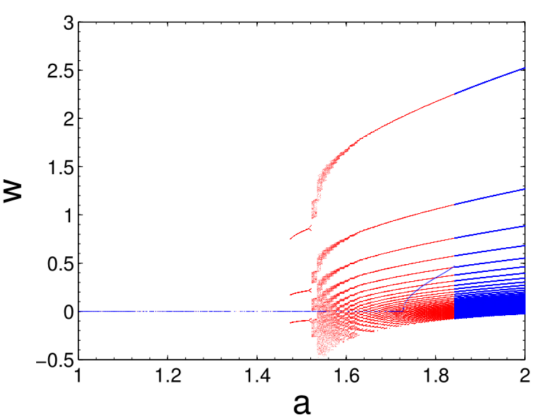

Fig. 1. Bifurcation diagrams of w versus a of system (1) plotted in the region $1 \leq a \leq 2$. Upward direction (Blue) and downward direction (red) with the IC $(0, 0, 0.1, 0.6)$ for $b = 0.54$, $f = 2.39$, $c = 0.54$, $d = 1.07$, $e = 1.97$.

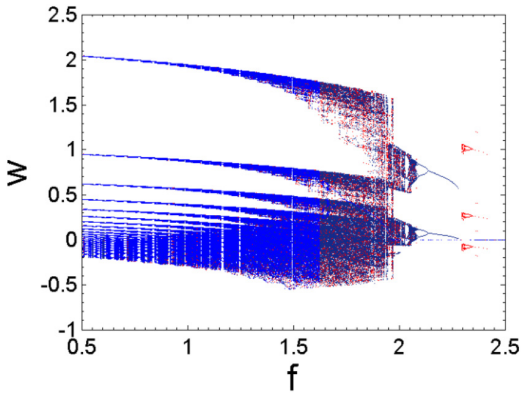

Fig. 2. Bifurcation diagrams of w versus f of system (1) plotted in the region $0.5 \leq f \leq 2.5$. Upward direction (Blue) and downward direction (black) with the IC $(0, 0, 0.1, 0.6)$. The graph in red is obtained by reinitializing the initial condition IC $= (0, 0, 0.1, 0.6)$. The remaining parameters are $b = 0.65$, $a = 1.55$, $c = 0.54$, $d = 1.07$, $e = 1.97$.

interval $1 \leq a \leq 2$. The graph in blue and red correspond to increasing and decreasing a, respectively. In Fig. 2, the bifurcation diagrams of the variable w versus f are obtained using three methods. The blue and black diagrams correspond to the upward and downward directions, respectively, while the graph in red is obtained with fixed initial points.

Similarly, Fig. 3(a) shows a bifurcation graph of the state variable x when varying a in the range $1.5 \leq a \leq 1.565$ and the corresponding graph of Lyapunov exponents [see Fig. 3(b)]. From Fig. 3, it is observed that the new hyper-jerk system develops a reverse period-doubling transition to chaos when parameter a slowly increased or decreased in the range $1.5 \leq a \leq 1.565$. Figure 4 demonstrates very well the transitions of the diagram provided in Fig. 3. That is, (a) period-1 limit cycle is plotted at $a = 1.5$, (b) period-2 limit cycle at $a = 1.53$, (c) period-4 limit cycle is shown for $a = 1.537$, (d) a strange hidden chaotic attractor is observed for $a = 1.55$, (e) period-4 limit cycle is obtained again for $a = 1.561$ and (f) period-2 attractor at $a = 1.565$. This sequence of behaviors found in the unique hyper-jerk system with a stable equilibrium also demonstrates the interesting path to chaos observed in many chaotic systems reported in the literature.

3.2. *Two-parameter Lyapunov exponents (LE)*

This section aims to investigate the general dynamics of the new hyper-jerk system (1). To gain more perception of the dynamics features and the performance of Eq. (1), two-parameter Lyapunov Exponents (LE) is provided. It is possible that the performance of the nonlinear systems also depends on the two-parameter LE diagram. The general dynamics behavior of the system is important for further application in engineering. The two-parameter graph also gives a possibility to use the oscillator in specific regions when parameters are changed simultaneously. In [Rech, 2017; Stegemann *et al.*, 2011], two-parameter LE is presented for chaotic or hyperchaotic systems to summarize their complex dynamical behavior. Two-parameter Lyapunov exponent is used to define a region of the possible existence of chaos or hyperchaos in the parameter space when two control bifurcations are changed simultaneously [Fonzin Fozin *et al.*, 2019]. In some situations, a two-parameter LE diagram

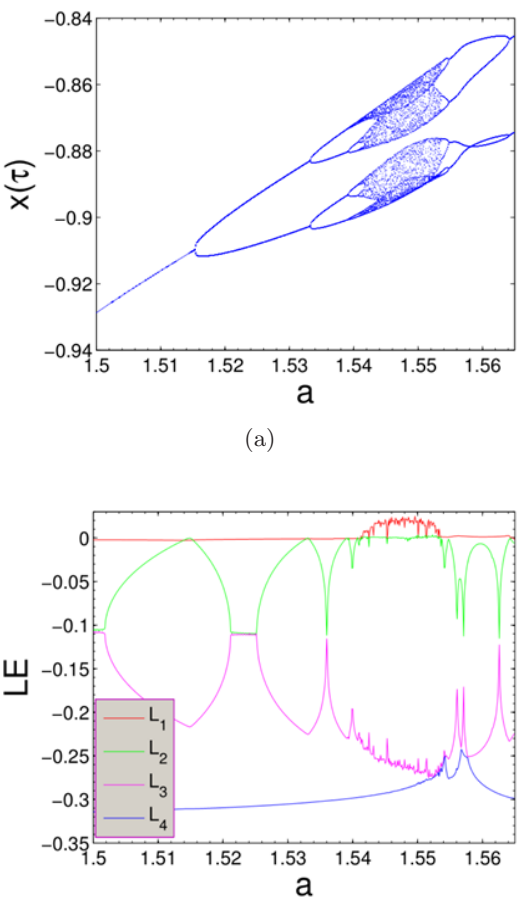

Fig. 3. Transition to chaos of parameter a in system (1): (a) Graph of bifurcation in the range $1.5 \leq a \leq 1.565$ and (b) Lyapunov exponent. IC is $(x(0), y(0), z(0), w(0)) = (-1.82, 0.2, 0.2, 0.5)$. $b = 0.54$,$f = 2.39$, $c = 0.53$, $d = 1.07$, $e = 1.97$.

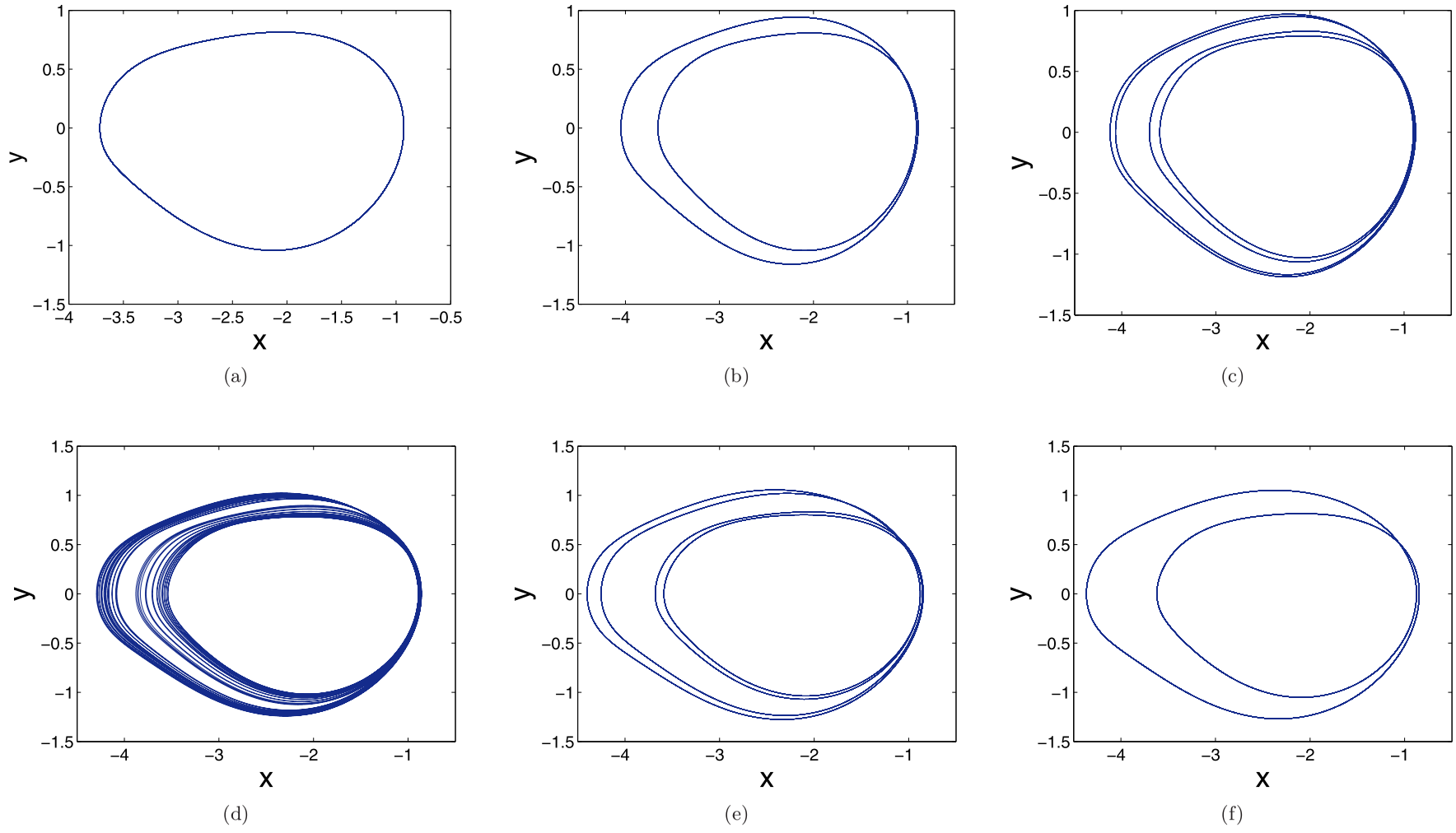

Fig. 4. Phase portrait of system (1) showing PD route to chaos by varying a: (a) Period-1 limit cycle for $a = 1.5$, (b) period-2 limit cycle for $a = 1.53$, (c) period-4 limit cycle for $a = 1.537$, (d) strange hidden chaotic attractor for $a = 1.55$, (e) period-4 limit attractor for $a = 1.561$ and (f) period-2 limit cycle for $a = 1.565$.

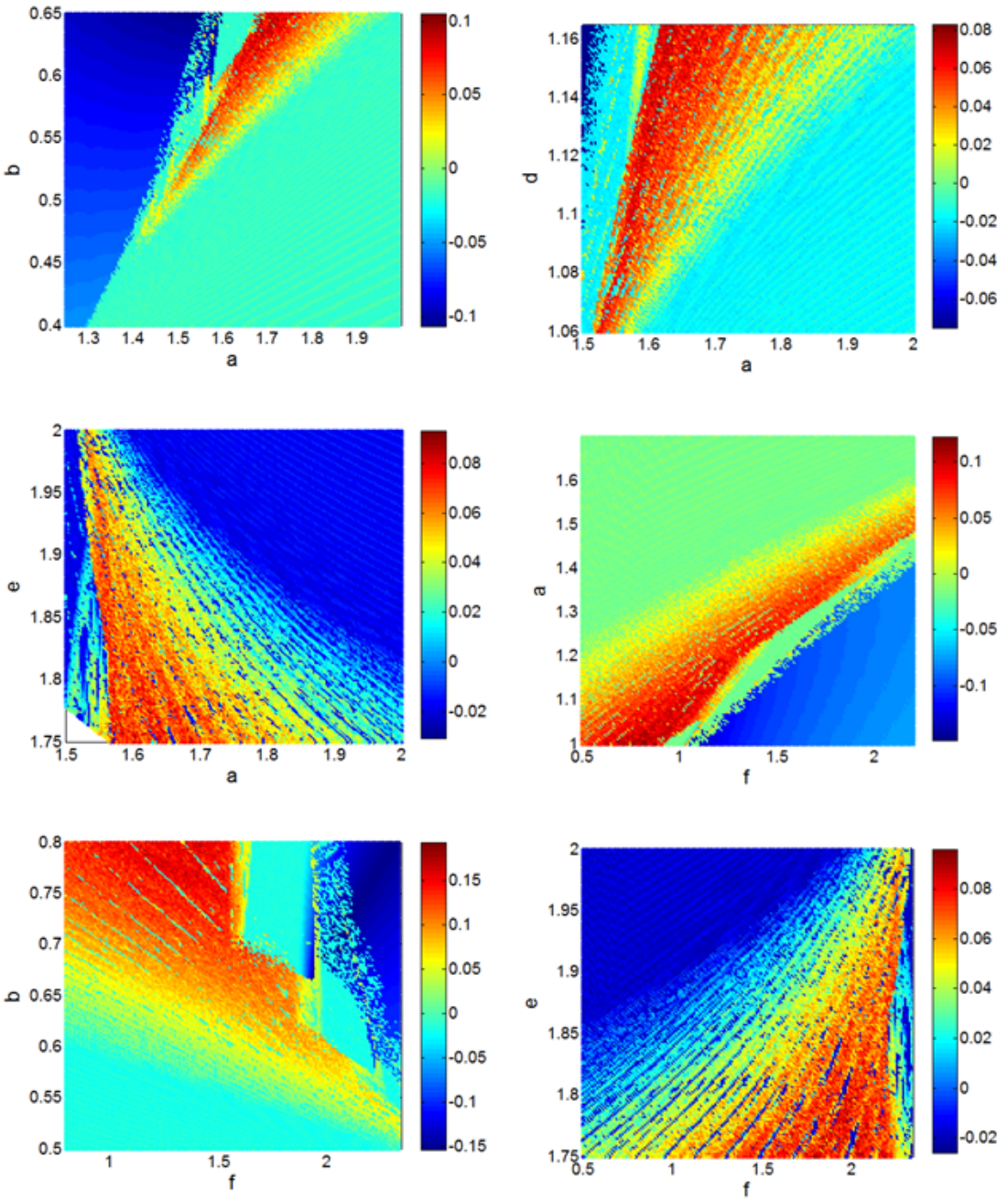

Fig. 5. Two-parameter LE diagrams showing different oscillation modes (chaotic or periodic modes) of the hyper-jerk system (1) in (a–b) plane when $f = 2.39$, $c = 0.54$, $d = 1.07$, $e = 1.97$; in (a–d) plane when $b = 0.54$, $f = 2.39$, $c = 0.54$, $e = 1.97$; in (a–e) plane with $b = 0.54$, $f = 2.39$, $c = 0.54$, $d = 1.07$; in (f–a) plane for $b = 0.54$, $c = 0.54$, $d = 1.07$, $e = 1.97$; in (f–b) plane for $a = 1.55$, $c = 0.54$, $d = 1.07$, $e = 1.97$, and in (f–e) plane for $b = 0.54$, $a = 1.55$, $c = 0.54$, $d = 1.07$. Initial point is $(0.1, 0, 0, 0)$.

is exploited to demonstrate different regions of coexisting attractors and coexisting bifurcations in the parameter space, as reported in [Negou & Kengne, 2019]. The two-parameter Lyapunov exponent (LE) defined in this paper present the general oscillation modes of the new hyper-jerk system when adjusting two control parameters. Indeed, two-parameter Lyapunov exponents (LE) are drawn by simultaneously adjusting two control parameters of the 4D system (1) through the establishment of appropriate colorful diagrams. The colorful graphs are obtained by numerically calculating the Lyapunov exponent spectrum using the algorithm proposed by the Wolf method [Wolf *et al.*, 1985], on a grid

time of 400×400 values of the chosen parameters. However, the two-parameter bifurcation diagram is directly associated with the two-parameter LE since it allows to distinguish the different oscillation zones such as periodic oscillations (i.e. negative LE) and chaotic oscillations (i.e. positive LE). In this paper, we present two-parameter Lyapunov exponent diagrams that help us find all these dynamic behaviors in the introduced hyper-jerk system. The dynamics of the introduced hidden oscillator are detailed as shown in Fig. 5 in different parameters space of Eq. (1). It can be seen from these graphs that when two control parameters are varied, chaotic and, regular oscillation modes can be distinguished in terms of the calculated LE value. For example, blue or Cyan shows negative or zero LE; a continuously changing green-yellow scale represents positive LE while the most positive LE is shown by red color.

3.3. *Coexisting bifurcation diagrams and multistability*

This part's main objective is to show the presence of a multitude of coexisting bifurcations and thus coexisting attractors in the new hyper-jerk system. The coexistence of many attractors strongly depends on the choice of initial conditions and parameter space. In addition, the coexistence of several solutions and thus multistability is carried out using bifurcation diagrams defined by sweeping the control parameters (i.e. upward and backward continuation). Clearly, exploiting the two-parameter diagrams presented in Fig. 5, for a discrete value of $b = 0.54$, $f = 2.39$, $c = 0.54$, $d = 1.07$, $e = 1.97$, and varying a in the appropriate range, the coexisting bifurcation diagrams are computed. These diagrams are obtained using the well-known continuation technique [Meli *et al.*, 2021; Tametang Meli *et al.*, 2021], where the final state of each iteration is used as the initial condition for the next iteration. Sample results show coexisting bifurcation of the new hyper-jerk oscillator as depicted in Figs. 6(a) and 6(b). This figure represents a zoom of the bifurcation diagram of Fig. 1 in the range $1.523 \leq a \leq 1.5325$. Each graph corresponds to increasing the control parameter a (see Fig. 6). These superimposed branches in Figs. 6(a) and 6(b) justify the coexistence of four different attractors in phase space, as shown in Figs. 7(a) and 7(b). That is a period-1 limit cycle attractor; a period-2 limit cycle and a strange chaotic attractor coexist with point attractor, as shown in Fig. 7(a).

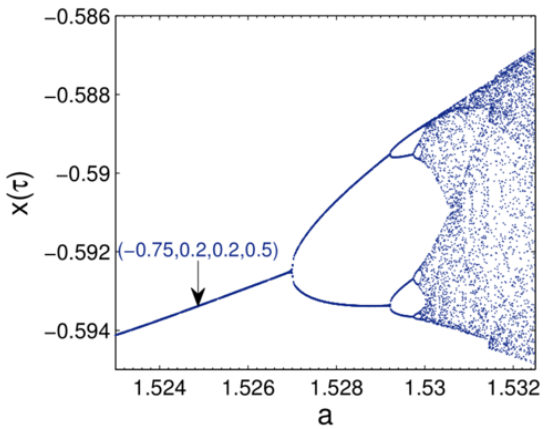

(a)

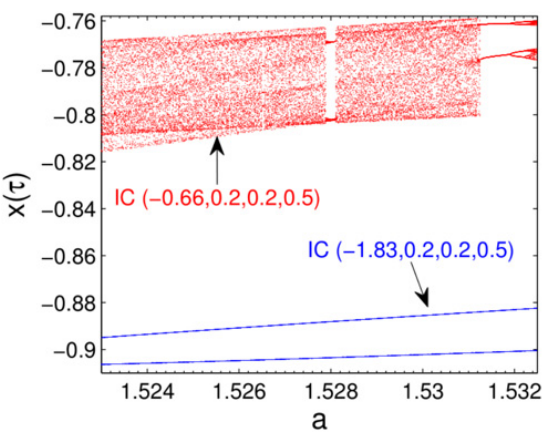

(b)

Fig. 6. Coexisting bifurcation diagrams obtained in the same regions of parameter a ($1.523 \leq a \leq 1.5325$) plotted in the upward direction with different ICs for $b = 0.54$, $f = 2.39$, $c = 0.54$, $d = 1.07$, $e = 1.97$.

In Fig. 7(b), two asymmetric period-2 limit cycles and an asymmetric strange attractor coexist with a point attractor.

Other zooms (see Figs. 8 and 10) of the bifurcation diagram of Fig. 6 are shown in Figs. 8 and 10, highlighting different dynamics of the hyper-jerk system. Up to four bifurcation branches coexist and can be used to explain different groups of coexisting attractors in the new oscillator. From the graphs in Fig. 8, four data correspond respectively to increase parameter a (see Table 3 for more details). Thus, the coexisting branches of Fig. 8 help to demonstrate the coexistence of many asymmetric attractors (up to five asymmetric attractors) in the new oscillator (see Fig. 9). It can be seen in Fig. 9(a) that two strange chaotic attractors, a period-1 limit cycle and a period-2 limit cycle, coexist with a point

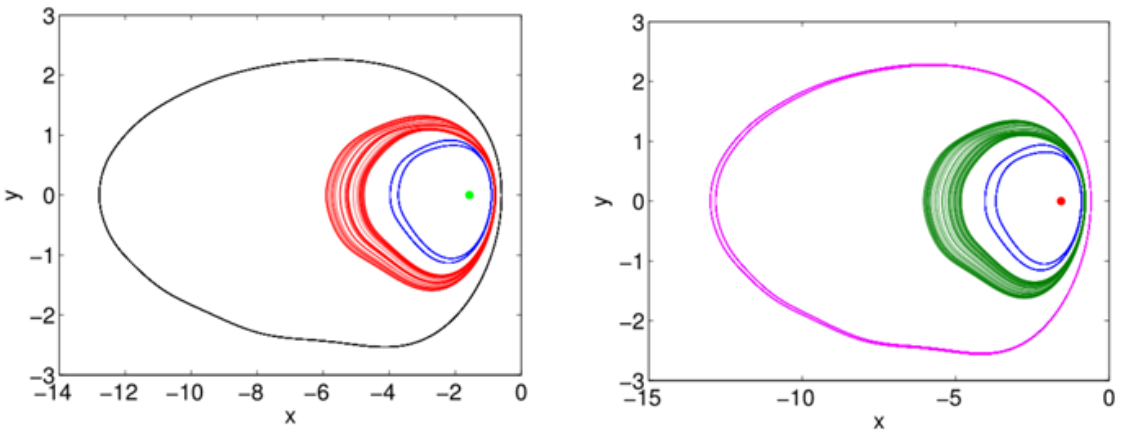

(a) (b)

Fig. 7. Coexistence of different attractors in system (1): (a) Period-1 attractor, period-2 attractor, chaotic attractor and point attractor for $a = 1.523$. IC1 (−1.83, 0.2, 0.2, 0.5), IC2 (−0.66, 0.2, 0.2, 0.5), IC3 (−0.75, 0.2, 0.2, 0.5), and IC4 (−2.5, 0.2, 0.2, 0.5) and (b) two period-2 attractors, a chaotic attractor and a point attractor for $a = 1.529$ with IC1 (−0.75, 0.2, 0.2, 0.5), IC2 (−0.66, 0.2, 0.2, 0.5), IC3 (−1.53, 0.2, 0.2, 0.5), and IC4 (−2.5, 0.2, 0.2, 0.5) respectively.

attractor under five distinct initial values. Also, two strange chaotic attractors coexist with asymmetric period-2 cycle, asymmetric period-4 cycle, and point attractor, as depicted in Fig. 9(b).

Similarly, Fig. 10 shows that coexisting branches can be exploited to justify the coexistence of four different asymmetric attractors without fixed-point attractors in the model. The method used to gain each diagram is summarized in Table 3 for more exploitation. These coexisting attractors can be periodic or chaotic. For example, by selecting four random initial values, two different asymmetric period-1 limit cycles coexist with two distinct strange attractors, as shown in Fig. 11(a). The situation where three different hidden chaotic attractors coexist with the period-1 limit cycle is highlighted in Fig. 11(b).

By using the same strategies, it is possible to track other coexisting branches and coexisting solutions. A strict analysis of the proposed hyperjerk system, based on Table 3 reveals other regions where parallel bifurcations coexist. The results of this analysis are shown in Fig. 12–14. In particular, the coexistence of several parallel bifurcation branches with hysteresis can be visualized in Fig. 12 (see Table 3 for more details). All these

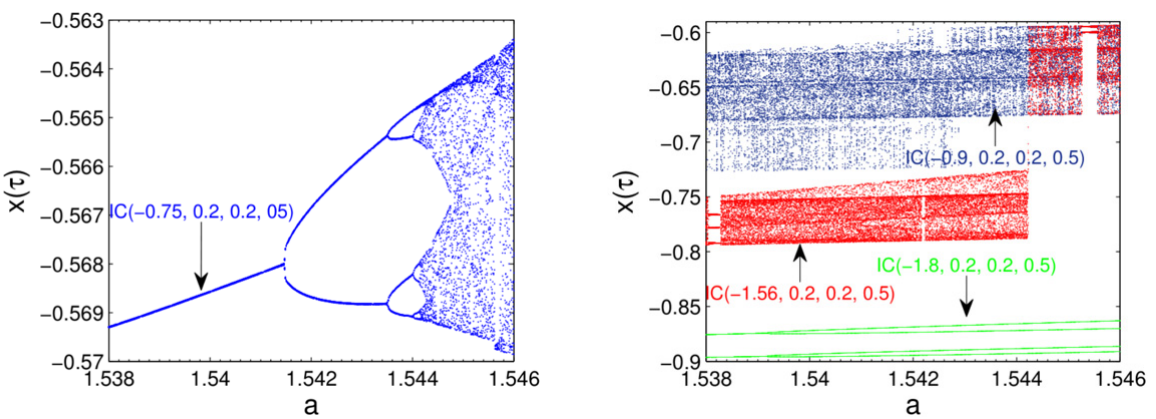

(a) (b)

Fig. 8. Coexisting bifurcation diagrams obtained in the same regions of parameter a ($1.538 \leq a \leq 1.546$) plotted in the upward direction with different ICs for $b = 0.54, f = 2.39, c = 0.54, d = 1.07, e = 1.97$. This figure helps to gain up to five different asymmetric coexisting attractors.

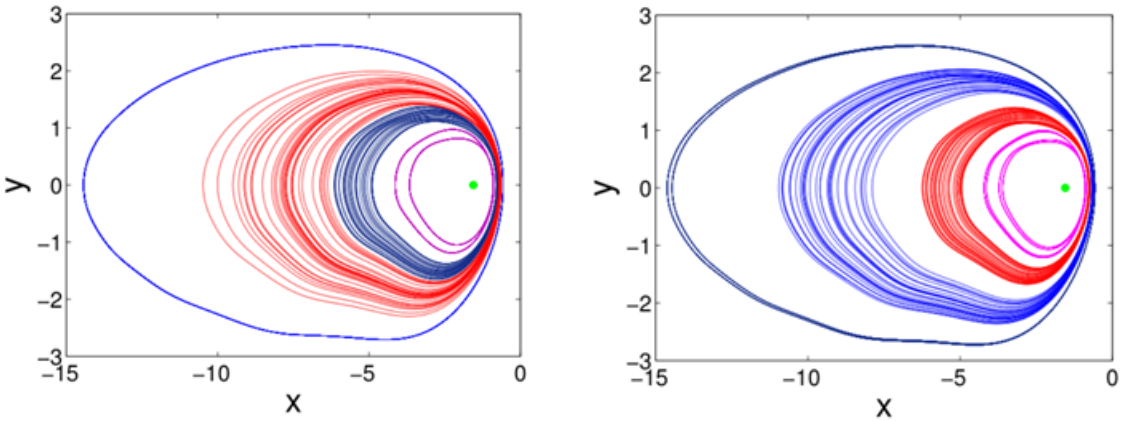

(a) (b)

Fig. 9. Coexistence of five different attractors with different shape including: (a) Period-1 attractor, period-2 attractor, two chaotic attractors and point attractor for $a = 1.538$ with ICs (−0.75, 0.2, 0.2, 0.5), (−1.8, 0.2, 0.2, 0.5), (−0.9, 0.2, 0.2, 0.5), (−1.56, 0.2, 0.2, 0.5), and (−2.5, 0.2, 0.2, 0.5) and (b) period-2 attractor, period-4 attractors, two asymmetric chaotic attractors and point attractor for $a = 1.543$ using ICs (−1.68, 0.2, 0.2, 0.5), (−1.98, 0.2, 0.2, 0.5), (−0.48, 0.2, 0.2, 0.5), (−1.29, 0.2, 0.2, 0.5), and (−2.5, 0.2, 0.2, 0.5), respectively.

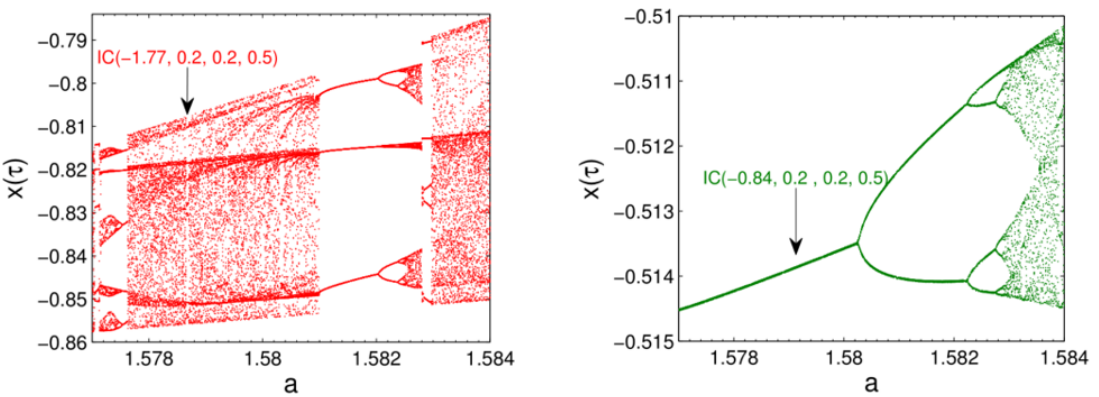

(a)

(b)

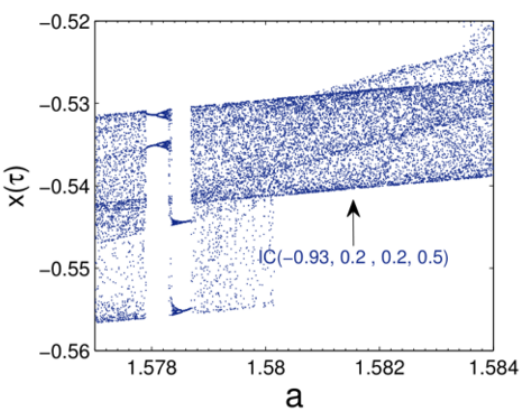

(c)

Fig. 10. Zoom diagram of Fig. 1 in the range $1.577 \leq a \leq 1.584$ plotted in the downward direction with different ICs. This figure shows the other coexisting solution region in the system (1).

Table 3. Procedures used to plot coexisting branches of Fig. 12. Other parameters are $b = 0.65$, $a = 1.55$,c=0.54, $d = 1.07$, $e = 1.97$.

Fig. No.	Color Graph	Parameter Range	Sweeping Direction	Initial Values $(x(0), y(0), z(0), w(0))$
12	Green	$2 \leq f \leq 2.364$	Decreasing	(0, 0, 0.1, 0.6)
	Black	$2 \leq f \leq 2.25$	Decreasing	(0, 0, 0.1, 0.24)
		$2.25 \leq f \leq 2.364$	Increasing	(0, 0, 0.1, 0.24)
	Red	$2 \leq f \leq 2.25$	Decreasing	(0, 0, 0.1, 0.36)
		$2.25 \leq f \leq 2.364$	Increasing	(0, 0, 0.1, 0.36)

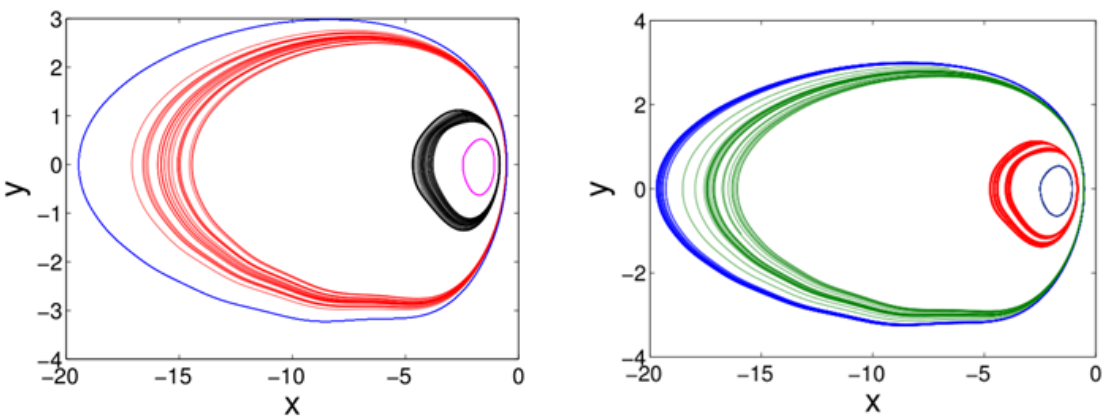

(a) (b)

Fig. 11. Coexistence of four different asymmetric attractors without any point attractor: (a) Period-1 attractor, and three asymmetric chaotic attractor for $a = 1.584$ with ICs $(-2.5, 0.2, 0.2, 0.5)$, $(-1.77, 0.2, 0.2, 0.5)$, $(-0.84, 0.2, 0.2, 0.5)$, and $(-0.93, 0.2, 0.2, 0.5)$ and (b) a pair of period-1 attractors, and a pair of chaotic attractors for $a = 1.579$ and ICs $(-0.45, 0.2, 0.2, 0.5)$, $(-2.5, 0.2, 0.2, 0.5)$, $(-1.8, 0.2, 0.2, 0.5)$, and $(-1.47, 0.2, 0.2, 0.5)$, respectively.

investigations demonstrate that the introduced hyper-jerk oscillator is capable of a plethora of coexisting behaviors. The demarcation region of initial values is defined to show different domains of some coexisting solutions. This demarcation region represents cross-sections of the basin of attraction in the different planes with other initial points fixed to zero, as shown in Fig. 15.

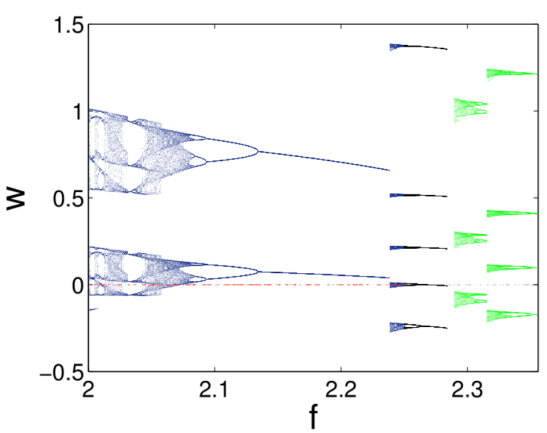

Fig. 12. Zoom diagram of Fig. 2 for the range of parameters $2 \leq f \leq 2.364$ plotted in the upward and downward directions with different ICs as summarized in Table 3.

3.4. *Control*

3.4.1. *Offset boosting control*

In general, offset boosting is used in nonlinear systems to shift chaotic signals or the basin of attraction in phase spaces. This interesting feature can be exploited to induce multistability (i.e. coexisting attractors) in dynamical systems. Also, one can break the symmetry of a dynamical system by introducing a boosting controller [Li *et al.*, 2020b; Lu *et al.*, 2019; Lu *et al.*, 2020]. A simple chaos generator of conditional symmetry induced by offset boosting is investigated using an efficient methodology of dynamics editing in [Li *et al.*, 2020a]. Using the transformation of the variable $x \to q + x$ and substituting it into the new hyper-jerk system given

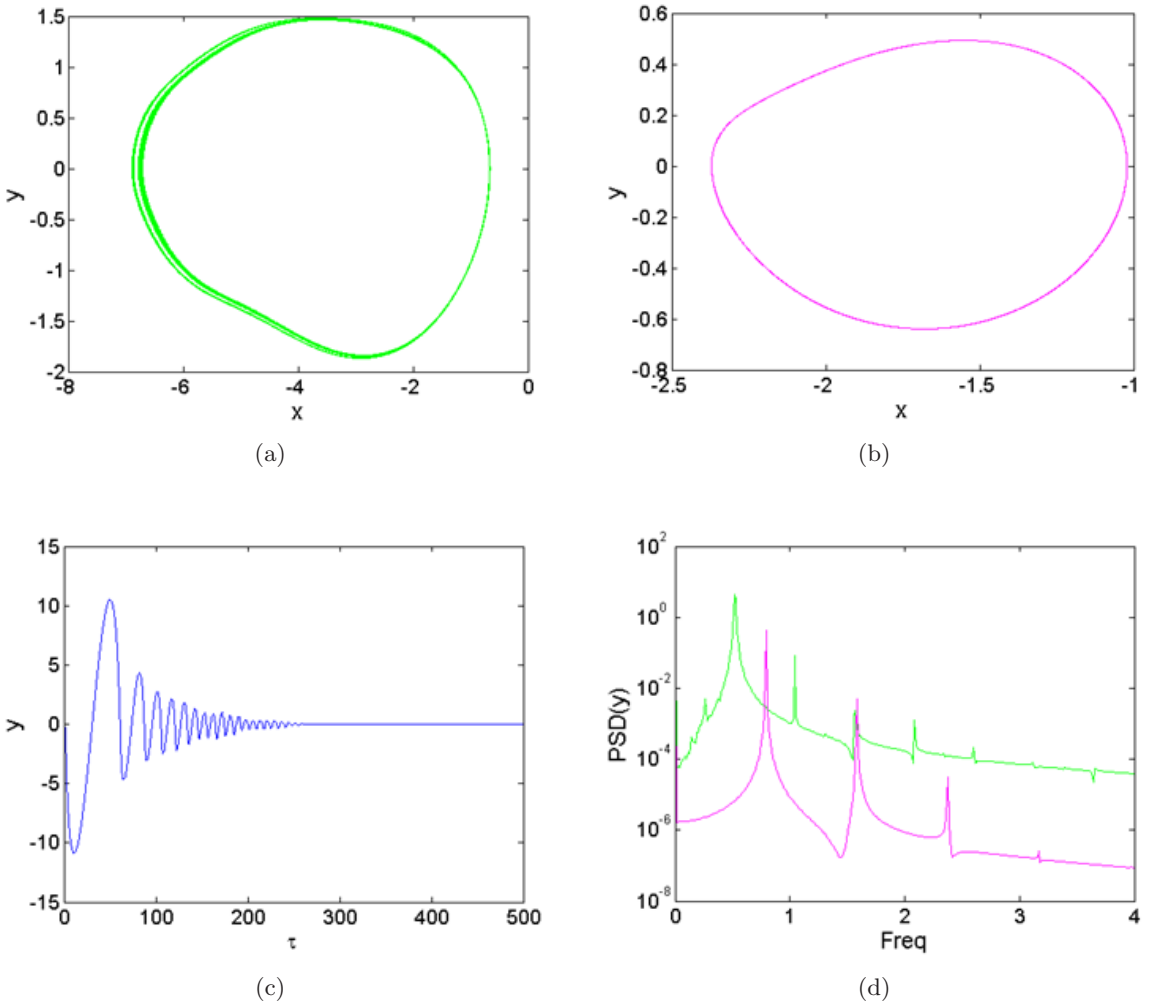

Fig. 13. Coexistence of three different attractors with different shapes, including (a) a pair of chaotic attractors, (b) period-1 attractor and point attractor illustrated by time series in (c) for $f = 2.25$. Initial conditions $(x(0), y(0), z(0), w(0))$ are (0, 0, 0.1, 0.24), (0, 0, 0.1, 0.28), and (0, 0, 0.1, 0.36) respectively. The frequency spectra of the chaotic and periodic attractors are represented in (d).

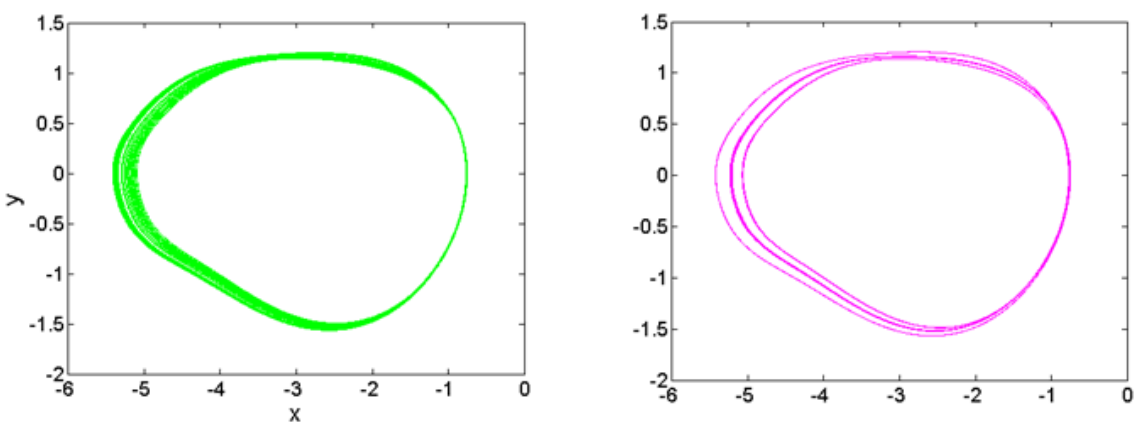

Fig. 14. Solutions coexist in the system (1) for $f = 2.323$ including (a) a chaotic attractor, (b) period-3 attractor and (c) period-2 attractor with IC1 (0, 0, 0.1, 0.28), IC2 (0, 0, 0.1, 0.38), and IC3 (0, 0, 0.1, 0.18), respectively, and their corresponding frequency spectra in (d).

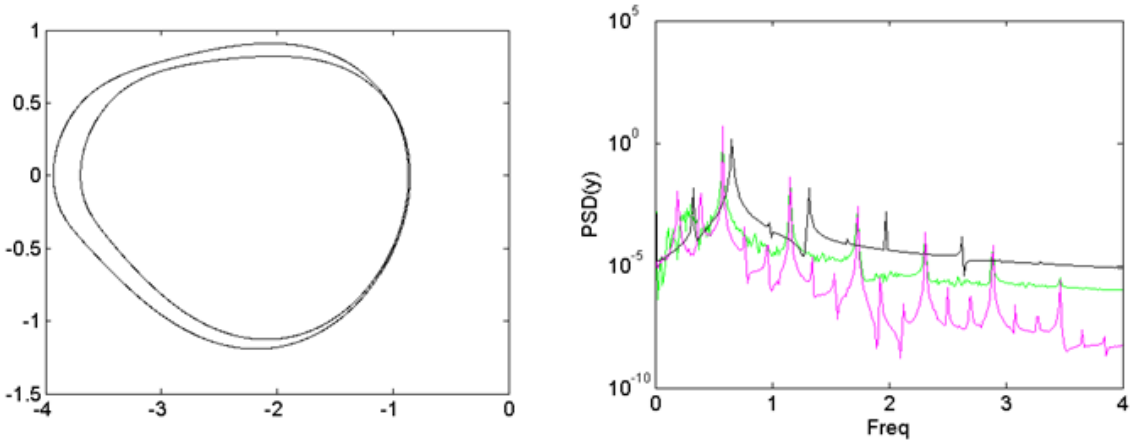

(c) (d)

Fig. 14. (*Continued*)

in Eq. (1), yields

$$\begin{cases} \dot{x} = y, \\ \dot{y} = z, \\ \dot{z} = w, \\ \dot{w} = -a(q+x) - by - cw - dy^2 \\ \qquad + e(q+x)z - f. \end{cases} \tag{7}$$

In Fig. 16, offset boosting is provided in (x, z) and (x, w) planes when adjusting the constant q. We observe that when $q > 0$, the chaotic signal x is shifted in the negative direction, and when $q < 0$, this chaotic signal shifts in the positive direction.

3.4.2. *Total amplitude control*

Consider the following transformation necessary to control the amplitude in the system (1):

$$x = \frac{1}{d}\hat{x}, \quad y = \frac{1}{d}\hat{y}, \quad z = \frac{1}{d}\hat{z}, \quad w = \frac{1}{d}\hat{w}. \tag{8}$$

When the transformation, given in Eq. (8), is applied to the nonlinear Eq. (1), we obtained the new 4D hyper-jerk system as follows:

$$\begin{cases} \dot{\hat{x}} = \hat{y}, \\ \dot{\hat{y}} = \hat{z}, \\ \dot{\hat{z}} = \hat{w}, \\ \dot{\hat{w}} = -a\hat{x} - b\hat{y} - c\hat{w} - \dfrac{\hat{y}^2}{d} + \dfrac{e\hat{x}\hat{z}}{d} - \dfrac{f}{d}. \end{cases} \tag{9}$$

One can remark that Eq. (9) is identical to Eq. (1) for $d = 1$. Thus, the constant term d in the 4D hyper-jerk oscillator can be exploited to control the amplitude of all variables proportionally and simultaneously according to $1/d$. This control technique is called total amplitude control (TAC) [Gu *et al.*, 2021; Leutcho *et al.*, 2021; Li & Sprott, 2014; Zang *et al.*, 2020] because all the states in the chaotic hyper-jerk system can be controlled when changing the coefficient d. The amplitude control of the strange chaotic attractor of the system (1) in different planes when changing d is shown in Fig. 17. In electronic circuit design, this amplitude coefficient can be realized using only a potentiometer.

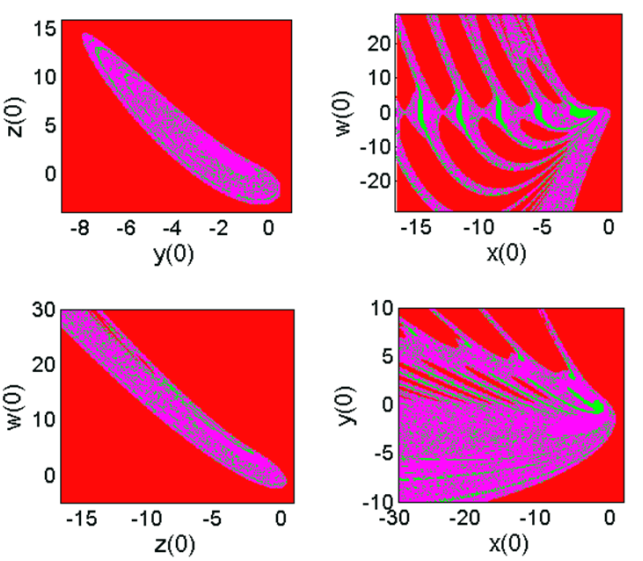

Fig. 15. Attraction domain in the different planes with other IC = 0: The magenta region is the zone where two chaotic attractors coexist while the domain of initial values (where the two period-1 limit cycles coexist) is represented in green. Parameters are $b = 0.54$, $a = 1.579$, $c = 0.54$, $d = 1.07$, $e = 1.97$, $f = 2.97$, respectively.

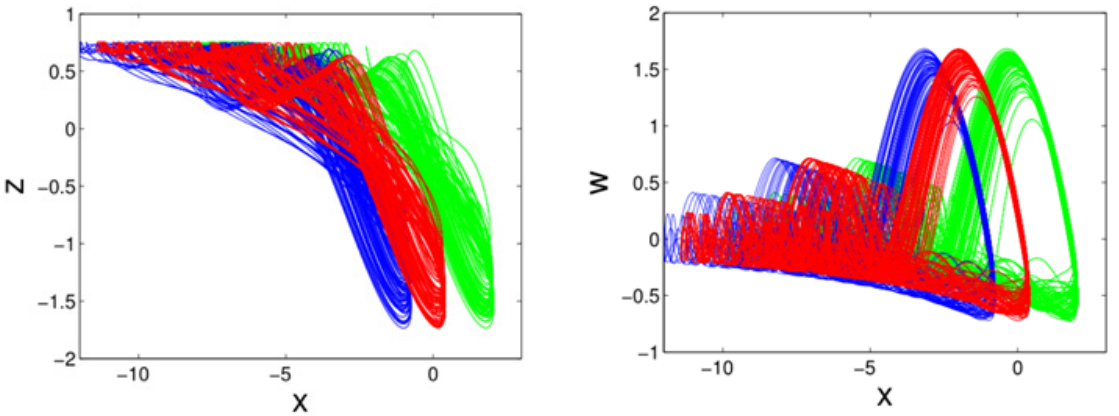

(a) (b)

Fig. 16. Offset boosting of the chaotic signal in the new hyper-jerk system for varying boostable states q as follows: Green attractor for $q = -2.5$, red attractor for $q = -0.86$, and blue attractor for $q = 0.3$. It is observed that chaotic signals can be moved through the x-axis. The initial point is (0, 0, 0.1, 0.18), and the rest of the parameters are those in Fig. 1.

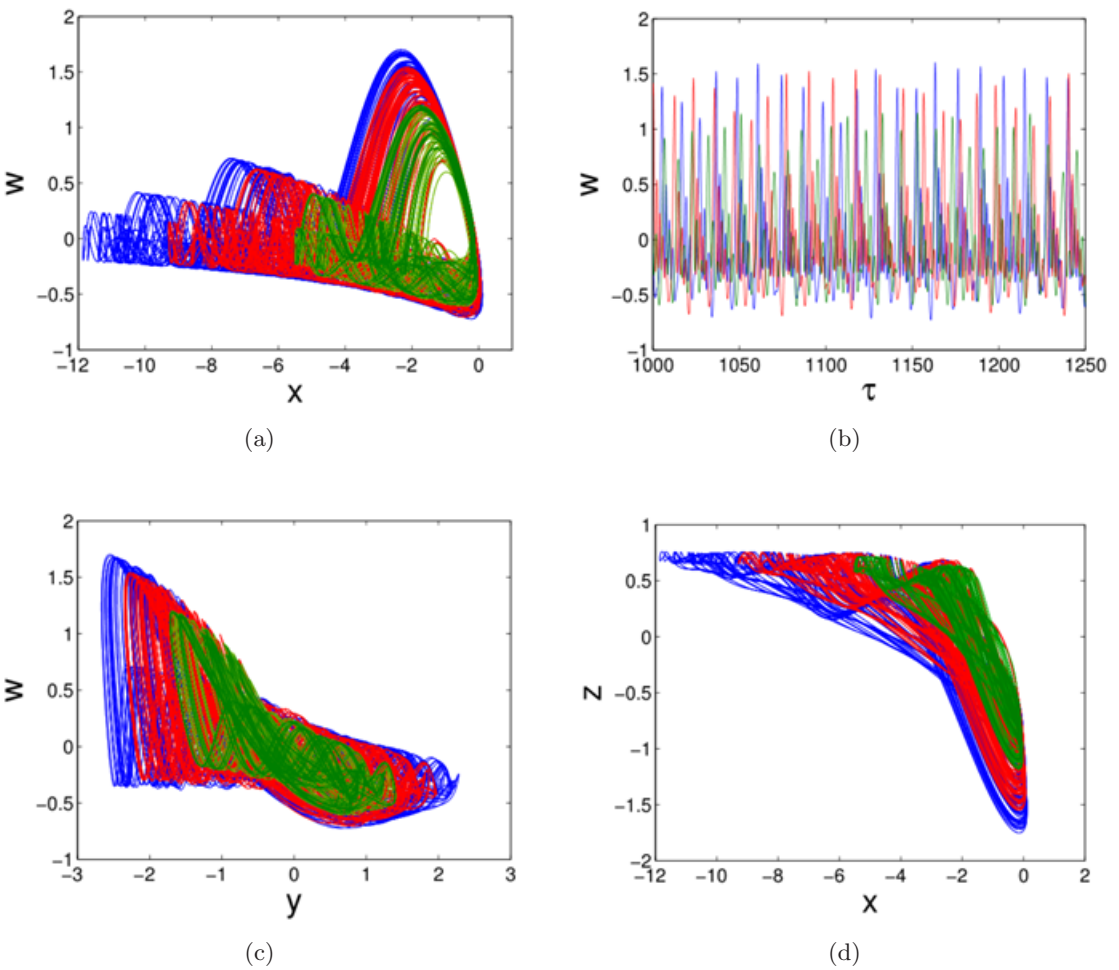

(a) (b)

(c) (d)

Fig. 17. (a)–(d) Amplitude control of the chaotic signal of system (1) plotted for $d = 1.065$ (blue), $d = 1.1$ (red) and $d = 1.22$ (yellow). IC (0, 0, 0.1, 0.18) and the rest of the parameters are those in Fig. 1.

3.5. *Antimonotonicity*

Let us emphasize that the birth of periodic orbits followed by their annihilation by an inverse PD transition when a control parameter is slowly modified is called an antimonotonicity [Kyprianidis *et al.*, 2000]. This interesting property has been investigated in many nonlinear systems, including laser systems [Parlitz & Lauterborn, 1985], Chua circuit [Dawson *et al.*, 1992], Duffing oscillator [Kengne *et al.*, 2018], and autonomous MLC oscillator [Kocarev *et al.*, 1993]. In 2018, the first exploration of antimonotonicity in 4D hyper-jerk circuits with hyperbolic sine nonlinearity was conducted [Leutcho *et al.*, 2018]. In [Leutcho *et al.*, 2020b], the authors proposed different bifurcations in which bubbles coexist in series or in parallel. Also, a chaotic bubble can coexist with a periodic bubble when the symmetric of a chaotic system is broken,

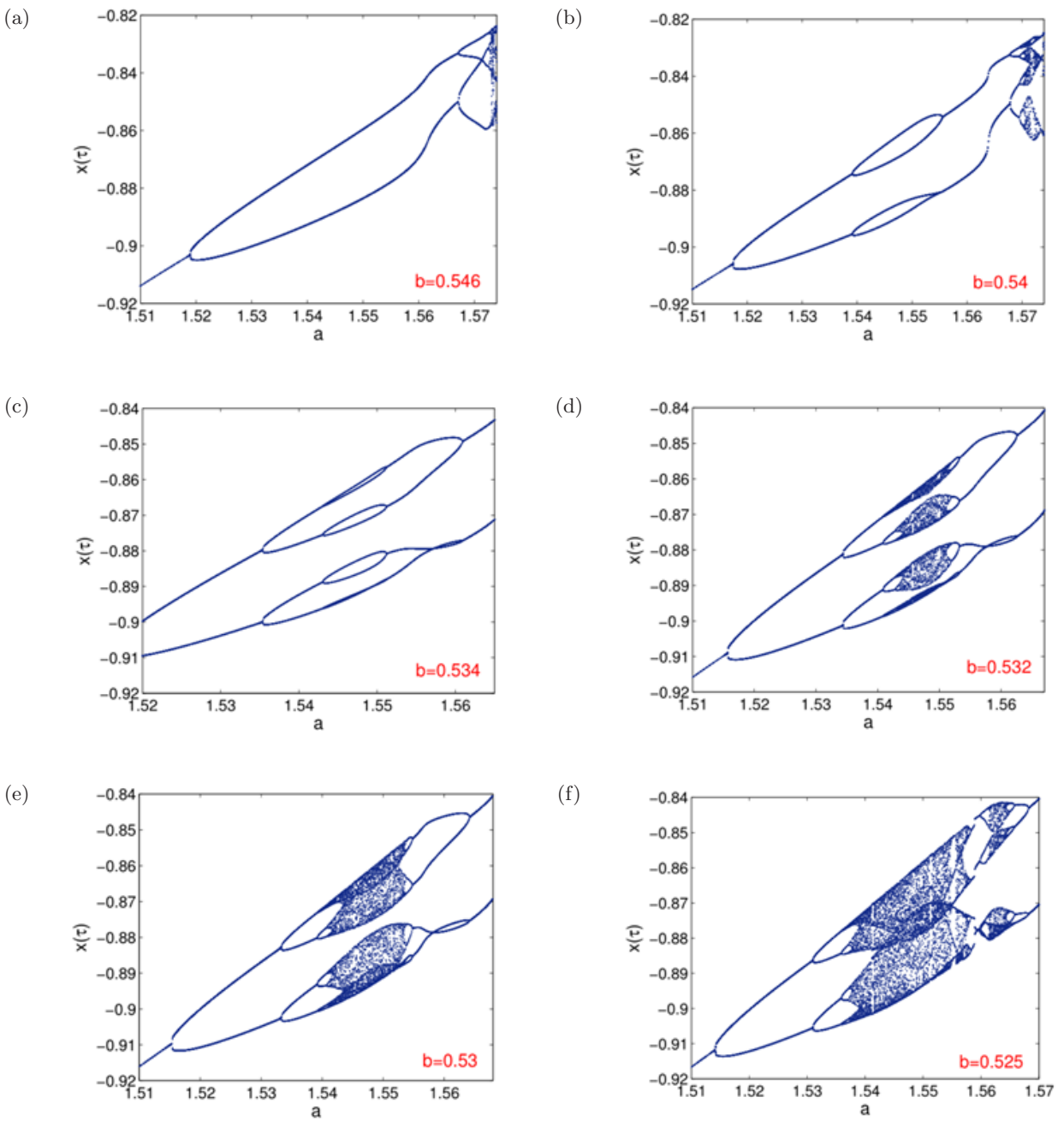

Fig. 18. Asymmetric bubbles of bifurcation computed for the same parameter setting in Fig. 1 in the range $1.51 \leq a \leq 1.57$ with initial conditions $(-1.82, 0.2, 0.2, 0.5)$ when scanning the parameter upward (continuation method).

as presented in [Kengne *et al.*, 2020a]. Recall beforehand that for a nonlinear system to change period-doubling bifurcations forward and backward, the presence of periodic islands in the parameter space is required [Negou & Kengne, 2019]. In Fig. 18, a sample result of antimonotonicity (i.e. asymmetric bubbles) in the new 4D hyper-jerk system for a specific parameter b is presented. For $b = 0.546$, period-2 bubble is obtained, at $b = 0.54$, period-4 bubble is formed, at $b = 0.534$, the bifurcation illustrates period-8 bubble. The first chaotic bubble is formed at $b = 0.532$. It is easy to see that the type of bubble changes when b is correctly chosen. As b is further decreased smoothly, more asymmetric bubbles are generated.

4. Design of the Circuit

PSIM (Power Simulation) is software used to design and simulate power electronics devices, motor, and order power devices. It can also be used to simulate simple electronic circuits based on conventional components. An interesting aspect of using such simulator software like PSIM based simulations (PSIM Professional Version 9.0.3.400 x32) is the possibility of easily introducing the initial state of the components like capacitor and inductor, thus in the wished case track the different coexisting attractor in the circuit. To achieve that goal, let us consider the electronic circuit depicted in Fig. 19. The circuit consists of components, such as operational amplifiers, capacitors, resistors, analogue devices AD633 multipliers.

Applying Kirchhoff's laws, the circuit of Fig. 19 is described by the following equations:

$$\begin{cases} \dfrac{dV_1}{dt} = \dfrac{1}{RC_1}V_2, \\ \dfrac{dV_2}{dt} = \dfrac{1}{RC_2}V_3, \\ \dfrac{dV_3}{dt} = \dfrac{1}{RC_3}V_4, \\ \dfrac{dV_4}{dt} = -\dfrac{1}{R_aC_4}V_1 - \dfrac{1}{R_bC_4}V_2 - \dfrac{1}{R_cC_4}V_4 \\ \qquad\qquad - \dfrac{1}{R_dC_4}V_2^2 + \dfrac{1}{R_eC_4}V_1V_3 - \dfrac{1}{R_fC_4}V_{cc}. \end{cases} \tag{10}$$

In order to avoid the saturation of the operational amplifiers, we reduce the scale of the amplitudes of the system by proceeding to the following change of variables:

$$V_1 = \frac{X}{10\,\mathrm{V}}; \quad V_2 = \frac{Y}{10\,\mathrm{V}}; \quad V_3 = \frac{Z}{10\,\mathrm{V}}; \quad V_4 = \frac{W}{10\,\mathrm{V}}. \tag{11}$$

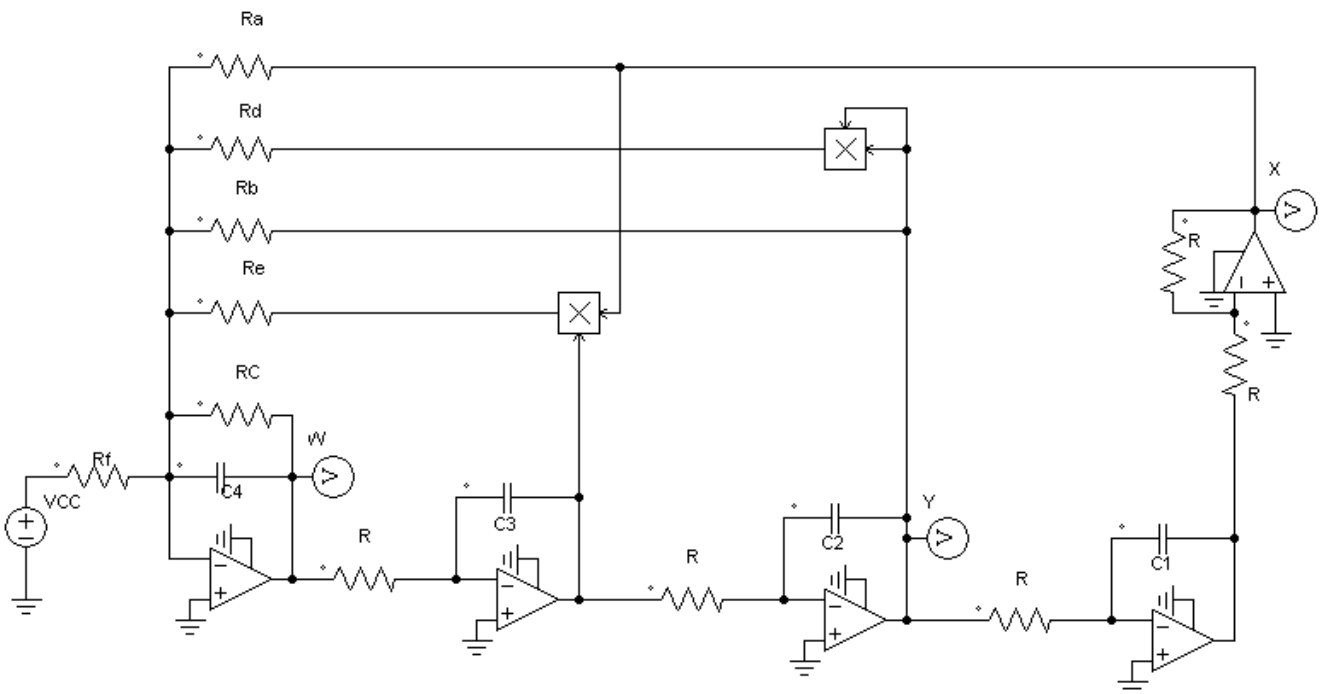

Fig. 19. Circuit realization of the new hyper-jerk system.

We obtained the following nonlinear four order differential equation:

$$\begin{cases} \dfrac{dX}{dt} = \dfrac{1}{RC_1}Y, \\ \dfrac{dY}{dt} = \dfrac{1}{RC_2}Z, \\ \dfrac{dZ}{dt} = \dfrac{1}{RC_3}W, \\ \dfrac{dW}{dt} = -\dfrac{1}{R_aC_4}X - \dfrac{1}{R_bC_4}Y - \dfrac{1}{R_cC_4}W \\ \qquad\quad - \dfrac{1}{10R_dC_4}Y^2 + \dfrac{1}{10R_eC_4}XZ - \dfrac{10}{R_fC_4}V_{cc}. \end{cases} \tag{12}$$

Choosing time changes as $t = \tau RC$ with $C = C_1 = C_2 = C_3 = C_4 = 10\,\text{nF}$ and $R = 10\,\text{K}\Omega$, the parameters of Eq. (1) are expressed in terms of the values of capacitors and resistors as follows:

$$\begin{aligned} \frac{R}{R_a} &= a; & \frac{R}{R_b} &= b; \\ \frac{R}{R_c} &= c; & \frac{R}{10R_d} &= d; \\ \frac{R}{10R_e} &= e; & \frac{10RV_{cc}}{10R_f} &= f. \end{aligned} \tag{13}$$

From Fig. 20, one can observe some sample number of attractors confirming the phenomenon of a large number of attractors observed during the numerical integration.

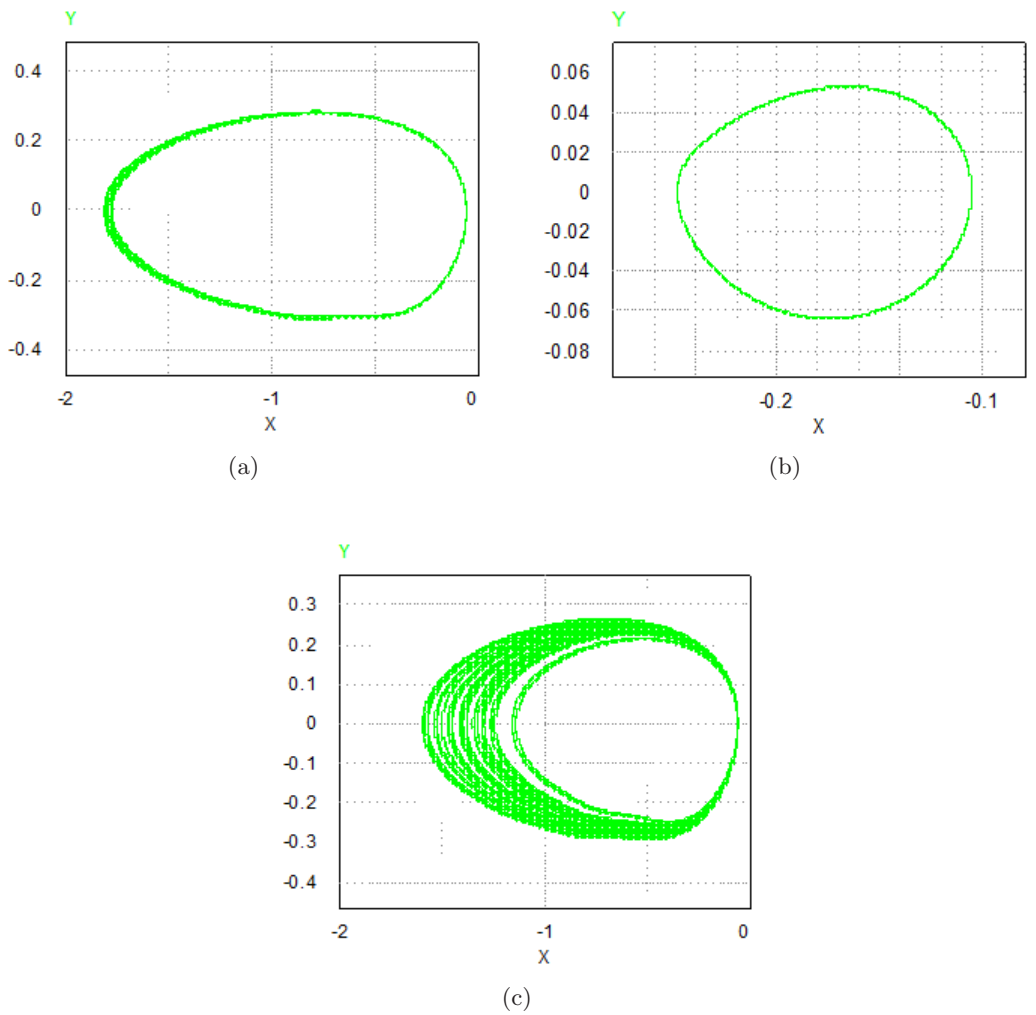

Fig. 20. PSIM based simulation result showing some of the coexisting attractors depicted in Fig. 10(a). This figure shows the coexistence of periodic attractors and one chaotic attractor with initial conditions $(x(0), y(0), z(0), w(0))$: $(-0.0247, 0.02, 0.03, 0.05)$, $(-0.2, 0.02, 0.08, 0.015)$, and $(-0.02, 0.02, 0.03, 0.05)$. The other resistors are fixed as $R_a = 6.337\,\text{K}\Omega$, $R_b = 18.52\,\text{K}\Omega$, $R_c = 18.52\,\Omega$, $R_d = 0.93\,\text{K}\Omega$, $R_e = 0.51\,\text{K}\Omega$, $R_f = 627.6\,\text{K}\Omega$.

5. Concluding Remarks

This contribution has focused on the dynamics of a new chaotic hyper-jerk system with a unique equilibrium. The nonlinear behavior observed in the newly introduced hyper-jerk system comes from two nonlinear quadratic terms. Based on the traditional nonlinear diagnostic tools such as bifurcation diagrams, phase portrait, frequency spectra, and two-parameter Lyapunov exponents, it has been found that the new hyper-jerk system effectively exhibits three types of hidden attractors, including hidden point attractor, hidden periodic attractor, and hidden chaotic attractor. The results indicate some interesting properties in the new hyper-jerk system, such as PD bifurcation, antimonotonicity, hysteretic dynamics, and coexisting strange attractors (up to five asymmetric hidden and self-excited attractors were found). The amplitude and offset of the hidden signals have been studied and perfectly controlled. Finally, the electronic analog of the model has been constructed and simulated in PSIM to confirm the occurrence of hidden behaviors.

Acknowledgment

This work is partially funded by Center for Materials Research, Chennai Institute of Technology, Chennai, India via funding number CIT/CMR/2021/RD/003.

References

Bao, H., Chen, C., Hu, Y., Chen, M. & Bao, B. [2020a] "2D piecewise-linear neuron model," *IEEE Trans. Circuits Syst.-II*: *Express Briefs* **68**, 1453–1457.

Bao, H., Hua, Z., Wang, N., Zhu, L., Chen, M. & Bao, B. [2020b] "Initials-boosted coexisting chaos in a 2D sine map and its hardware implementation," *IEEE Trans. Industr. Inform.* **17**, 1132–1140.

Chen, M., Sun, M., Bao, H., Hu, Y. & Bao, B. [2019] "Flux-charge analysis of two-memristor-based Chua's circuit: Dimensionality decreasing model for detecting extreme multistability," *IEEE Trans. Industr. Electron.* **67**, 2197–2206.

Chen, M., Wang, C., Bao, H., Ren, X., Bao, B. & Xu, Q. [2020] "Reconstitution for interpreting hidden dynamics with stable equilibrium point," *Chaos Solit. Fract.* **140**, 110188.

Dawson, S. P., Grebogi, C., Yorke, J. A., Kan, I. & Koçak, H. [1992] "Antimonotonicity: Inevitable reversals of period-doubling cascades," *Phys. Lett. A* **162**, 249–254.

Fonzin Fozin, T., Megavarna Ezhilarasu, P., Njitacke Tabekoueng, Z., Leutcho, G., Kengne, J., Thamilmaran, K., Mezatio, A. & Pelap, F. [2019] "On the dynamics of a simplified canonical Chua's oscillator with smooth hyperbolic sine nonlinearity: Hyperchaos, multistability and multistability control," *Chaos* **29**, 113105.

Fouodji Tsotsop, M., Kengne, J., Kenne, G. & Tabekoueng Njitacke, Z. [2020] "Coexistence of multiple points, limit cycles, and strange attractors in a simple autonomous hyperjerk circuit with hyperbolic sine function," *Complexity* **2020**, 6182183-1–24.

Giakoumis, A., Volos, C., Khalaf, A. J. M., Bayani, A., Stouboulos, I., Rajagopal, K. & Jafari, S. [2020] "Analysis, synchronization and microcontroller implementation of a new quasiperiodically forced chaotic oscillator with megastability," *Iranian J. Sci. Technol. Trans. Electric. Engin.* **44**, 31–45.

Gu, J., Li, C., Lei, T., He, S. & Min, F. [2021] "A memristive chaotic system with flexible attractor growing," *The European Phys. J.*: *Special Topics*, 1–14.

He, S., Li, C., Sun, K. & Jafari, S. [2018] "Multivariate multiscale complexity analysis of self-reproducing chaotic systems," *Entropy* **20**, 556.

Hu, D., Hu, L. & Yan, Y. [2018a] "Optimization methodology for control strategy of parallel hybrid electric vehicle based on chaos prediction," *AIP Advances* **8**, 115305.

Hu, D., Yan, Y. & Xu, X. [2018b] "Determination methodology for stable control domain of electric powertrain based on permanent magnet synchronous motor," *Adv. Mech. Engin.* **10**, 1687814018793053.

Jafari, S., Rajagopal, K., Hayat, T., Alsaedi, A. & Pham, V.-T. [2019] "Simplest megastable chaotic oscillator," *Int. J. Bifurcation and Chaos* **29**, 1950187-1–9.

Kengne, J., Signing, V. F., Chedjou, J. & Leutcho, G. [2018] "Nonlinear behavior of a novel chaotic jerk system: Antimonotonicity, crises, and multiple coexisting attractors," *Int. J. Dyn. Contr.* **6**, 468–485.

Kengne, L. K., Kengne, J. & Pone, J. R. M. [2020a] "Coexisting bubbles, multiple attractors, and control of multistability in a simple jerk system under the influence of a constant excitation force," *Pramana* **94**, 1–25.

Kengne, L. K., Tagne, H. K., Pone, J. M. & Kengne, J. [2020b] "Dynamics, control and symmetry-breaking aspects of a new chaotic jerk system and its circuit implementation," *The European Phys. J. Plus* **135**, 1–28.

Kocarev, L., Halle, K. S., Eckert, K. & Chua, L. O. [1993] "Experimental observation of antimonotonicity

in Chua's circuit," *Int. J. Bifurcation and Chaos* **3**, 1051–1055.

Kyprianidis, I. M., Stouboulos, I. N., Haralabidis, P. & Bountis, T. [2000] "Antimonotonicity and chaotic dynamics in a fourth-order autonomous nonlinear electric circuit," *Int. J. Bifurcation and Chaos* **10**, 1903–1915.

Leonov, G. A. & Kuznetsov, N. V. [2013] "Hidden attractors in dynamical systems. From hidden oscillations in Hilbert–Kolmogorov, Aizerman, and Kalman problems to hidden chaotic attractor in Chua circuits," *Int. J. Bifurcation and Chaos* **23**, 1330002-1–69.

Leonov, G. A., Kuznetsov, N. V. & Mokaev, T. N. [2015] "Hidden attractor and homoclinic orbit in Lorenz-like system describing convective fluid motion in rotating cavity," *Commun. Nonlin. Sci. Numer. Simulat.* **28**, 166–174.

Leutcho, G., Kengne, J. & Kengne, L. K. [2018] "Dynamical analysis of a novel autonomous 4D hyperjerk circuit with hyperbolic sine nonlinearity: Chaos, antimonotonicity and a plethora of coexisting attractors," *Chaos Solit. Fract.* **107**, 67–87.

Leutcho, G. D., Kengne, J., Fonzin Fozin, T., Srinivasan, K., Njitacke Tabekoueng, Z., Jafari, S. & Borda, M. [2020a] "Multistability control of space magnetization in hyperjerk oscillator: A case study," *J. Comput. Nonlin. Dyn.* **15**, 051004.

Leutcho, G. D., Kengne, J., Kengne, L. K., Akgul, A., Pham, V.-T. & Jafari, S. [2020b] "A novel chaotic hyperjerk circuit with bubbles of bifurcation: Mixed-mode bursting oscillations, multistability, and circuit realization," *Physica Scripta* **95**, 075216.

Leutcho, G. D., Wang, H., Kengne, R., Kengne, L. K., Njitacke, Z. T. & Fozin, T. F. [2021] "Symmetry-breaking, amplitude control and constant Lyapunov exponent based on single parameter snap flows," *The European Phys. J.: Special Topics*, 1–17.

Li, C. & Sprott, J. [2014] "Finding coexisting attractors using amplitude control," *Nonlin. Dyn.* **78**, 2059–2064.

Li, C., Lei, T., Wang, X. & Chen, G. [2020a] "Dynamics editing based on offset boosting," *Chaos* **30**, 063124.

Li, C., Sprott, J. C. & Liu, Y. [2020b] "Time-reversible chaotic system with conditional symmetry," *Int. J. Bifurcation and Chaos* **30**, 2050067-1–16.

Lu, T., Li, C., Jafari, S. & Min, F. [2019] "Controlling coexisting attractors of conditional symmetry," *Int. J. Bifurcation and Chaos* **29**, 1950207-1–16.

Lu, T., Li, C., Wang, X., Tao, C. & Liu, Z. [2020] "A memristive chaotic system with offset-boostable conditional symmetry," *The European Phys. J.: Special Topics* **229**, 1059–1069.

Malasoma, J.-M. [2000] "What is the simplest dissipative chaotic jerk equation which is parity invariant?" *Phys. Lett. A* **264**, 383–389.

Meli, M. I. T., Yemélé, D. & Leutcho, G. D. [2021] "Dynamical analysis of series hybrid electric vehicle powertrain with torsional vibration: Antimonotonicity and coexisting attractors," *Chaos Solit. Fract.* **150**, 111174.

Munmuangsaen, B. & Srisuchinwong, B. [2011] "Elementary chaotic snap flows," *Chaos Solit. Fract.* **44**, 995–1003.

Nana, B., Yamgoue, S. B., Tchitnga, R. & Woafo, P. [2018] "On the modeling of the dynamics of electrical hair clippers," *Chaos Solit. Fract.* **112**, 14–23.

Negou, A. N. & Kengne, J. [2019] "A minimal three-term chaotic flow with coexisting routes to chaos, multiple solutions, and its analog circuit realization," *Anal. Integr. Circuits Sign. Process.* **101**, 415–429.

Parlitz, U. & Lauterborn, W. [1985] "Superstructure in the bifurcation set of the duffing equation $\ddot{x} + d\dot{x} + x + x3 = f\cos(\omega t)$," *Phys. Lett. A* **107**, 351–355.

Pham, V.-T., Jafari, S., Kapitaniak, T., Volos, C. & Kingni, S. T. [2017] "Generating a chaotic system with one stable equilibrium," *Int. J. Bifurcation and Chaos* **27**, 1750053-1–8.

Rech, P. C. [2017] "Hyperchaos and quasiperiodicity from a four-dimensional system based on the Lorenz system," *The European Phys. J. B* **90**, 1–7.

Ren, S., Panahi, S., Rajagopal, K., Akgul, A., Pham, V.-T. & Jafari, S. [2018] "A new chaotic flow with hidden attractor: The first hyperjerk system with no equilibrium," *Zeitschrift für Naturforschung A* **73**, 239–249.

Singh, J., Pham, V., Hayat, T., Jafari, S., Alsaadi, F. & Roy, B. [2018] "A new four-dimensional hyperjerk system with stable equilibrium point, circuit implementation, and its synchronization by using an adaptive integrator backstepping control," *Chinese Phys. B* **27**, 100501.

Stegemann, C., Albuquerque, H. A., Rubinger, R. M. & Rech, P. C. [2011] "Lyapunov exponent diagrams of a 4-dimensional Chua system," *Chaos* **21**, 033105.

Strogatz, S. [1994] *Nonlinear Dynamics and Chaos* (Addison Wesley, Reading, MA).

Tametang Meli, M. I., Leutcho, G. D. & Yemele, D. [2021] "Multistability analysis and nonlinear vibration for generator set in series hybrid electric vehicle through electromechanical coupling," *Chaos* **31**, 073126.

Wang, X. & Chen, G. [2012] "A chaotic system with only one stable equilibrium," *Commun. Nonlin. Sci. Numer. Simulat.* **17**, 1264–1272.

Wolf, A., Swift, J. B., Swinney, H. L. & Vastano, J. A. [1985] "Determining Lyapunov exponents from a time series," *Physica D* **16**, 285–317.

Yu, Y., Shi, M., Kang, H., Chen, M. & Bao, B. [2020] "Hidden dynamics in a fractional-order memristive Hindmarsh–Rose model," *Nonlin. Dyn.* **100**, 891–906.

Zambrano-Serrano, E. & Anzo-Hernández, A. [2021] "A novel antimonotic hyperjerk system: Analysis, synchronization and circuit design," *Physica D* **424**, 132927.

Zang, H., Gu, Z., Lei, T., Li, C. & Jafari, S. [2020] "Coexisting chaotic attractors in a memristive system and their amplitude control," *Pramana* **94**, 1–9.

Zhang, Y., Liu, Z., Wu, H., Chen, S. & Bao, B. [2019] "Two-memristor-based chaotic system and its extreme multistability reconstitution via dimensionality reduction analysis," *Chaos Solit. Fract.* **127**, 354–363.